

See discussions, stats, and author profiles for this publication at:  
<https://www.researchgate.net/publication/15063615>

# Exogenous Acetate Reconstitutes the Enzymic Activity of Trypsin Asp189Ser

ARTICLE *in* BIOCHEMISTRY · APRIL 1994

Impact Factor: 3.02 · DOI: 10.1021/bi00177a016 · Source: PubMed

---

CITATIONS

43

---

READS

14

## 6 AUTHORS, INCLUDING:



John Perona  
Portland State University

90 PUBLICATIONS 3,493 CITATIONS

[SEE PROFILE](#)



Charles S Craik  
University of California, San Francisco  
332 PUBLICATIONS 15,161 CITATIONS

[SEE PROFILE](#)

# Exogenous Acetate Reconstitutes the Enzymatic Activity of Trypsin Asp189Ser<sup>†</sup>

John J. Perona,<sup>‡</sup> Lizbeth Hedstrom,<sup>||</sup> Richard L. Wagner,<sup>§</sup> William J. Rutter,<sup>⊥</sup> Charles S. Craik,<sup>†</sup> and Robert J. Fletterick\*,<sup>§</sup>

Departments of Pharmaceutical Chemistry and Biochemistry & Biophysics and Hormone Research Institute,  
University of California, San Francisco, California 94143-0446

Received September 15, 1993; Revised Manuscript Received December 17, 1993\*

**ABSTRACT:** The specificity of trypsin for Arg- and Lys-containing substrates depends upon the presence of Asp189 at the base of the primary binding pocket. The crystal structure of anionic rat trypsin D189S complexed with BPTI reveals that removal of the aspartate side chain permits the binding of a well-ordered acetate ion in a similar position. The acetate makes polar interactions with Gly226, Tyr228, and several water molecules and is further accommodated by rotation of the Ser189 side chain out of the binding pocket. The carboxylate group of the acetate anion is oriented toward the substrate in a manner similar to that of Asp189 and Asp226 in wild-type trypsin and trypsin D189G/G226D. Evaluation of kinetic parameters for amide substrate cleavage by trypsin D189S shows that high concentrations of acetate increase the catalytic efficiency of the enzyme by as much as 300-fold. Under these conditions, the rate of substrate turnover toward a peptidylarginine amide substrate equals that of wild-type trypsin. These data demonstrate that the well-established requirement for a negatively charged moiety at the base of the trypsin specificity pocket may be fulfilled by a noncovalently bound ligand. The binding pocket of this variant maintains a trypsin-like conformation, explaining the inability of the mutant enzyme to efficiently hydrolyze chymotrypsin substrates possessing Phe in the P1 position.

A recent theme in the investigation of enzyme catalysis is the restoration of activity attenuated by the deletion of specific amino acid side chains, via the addition of small molecules. Exogenous amines restored activity to a mutant aspartate aminotransferase lacking the catalytic lysine residue (Toney & Kirsch, 1989), while the addition of guanidine derivatives partially reconstituted the activity of a mutant carboxypeptidase, from which the Arg127 side chain was removed (Phillips et al., 1992). Similarly, aminomethanesulfonate restored activity to a mutant ribulosebisphosphate carboxylase/oxygenase lacking a catalytic lysine amino acid (Smith & Hartman, 1991), and exogenous imidazole caused an increase in the  $k_{cat}$  of H64A subtilisin by 20-fold (Carter et al., 1991). In each case, chemical rescue was applied to a group that participates directly in the bond-making or bond-breaking steps of catalysis. In a nonenzymic context, rhodopsin mutants were studied in which the side chain of a lysine residue forming a Schiff base linkage to the retinal chromophore was deleted (Zhukovsky et al., 1991). Exogenously added chromophore bound and activated transducin when linked with an *n*-alkylamine through a Schiff base linkage.

Trypsin specifically cleaves peptide bonds adjacent to Arg and Lys residues. Crystallographic studies have suggested that this specificity arises from the presence of Asp189 at the base of the binding pocket, where it provides a negatively charged electrostatic field (Ruhmann et al., 1973; Krieger et al., 1974). More recently, mutational analysis has confirmed that removal of this negatively charged carboxylate reduces activity by at least a factor of 10<sup>4</sup> (Graf et al., 1988; Evnin

et al., 1990). However, activity could be partially restored by the introduction of a negatively charged group at position 190 or 226 (Evnin et al., 1990; Perona et al., 1993b, 1994). This observation indicates that the presence of a negative electrostatic potential at the base of the binding pocket is in itself sufficient to provide specific rate enhancement toward Arg and Lys substrates. However, precise positioning of the carboxylate group is critical to achieving optimal catalytic efficiency.

Anionic rat trypsin D189S lacks a negatively charged group in its specificity pocket and consequently exhibits poor activity toward Lys- and Arg-containing substrates (Graf et al., 1988). This mutation replaces Asp189 with the analogous Ser residue of chymotrypsin, a homologous protease which manifests specificity for large hydrophobic amino acids and which possesses a substrate binding pocket that is similar, but not identical, in size and shape. The mutation of Asp189 to Ser is sufficient to convert trypsin into a chymotrypsin-like esterase. However, the trypsin-catalyzed hydrolysis of amide substrates containing Phe at position P1 is not significantly improved by the D189S mutation. Trypsin D189S also does not utilize binding of the extended peptide in the P2-P4 sites to accelerate the hydrolysis of amide substrates containing Phe at position P1 (Hedstrom et al., 1992; see Figure 2 legend for subsite nomenclature). Conversion of trypsin into a chymotrypsin-like amidase has been shown to require substitution of four amino acids in the S1 pocket as well as the exchange of two adjacent surface loops (Hedstrom et al., 1992).

To address the structural basis for the kinetic properties of trypsin D189S, we have determined its crystal structure bound

\* This work was supported by NSF Grant DMB9219806 (to C.S.C.), NIH Grant DK39304 (to R.J.F.), NIH Grant DK21344 (to W.J.R.), and NIH Postdoctoral NRSA Award GM13818-03 (to J.J.P.).

† Department of Pharmaceutical Chemistry.

|| Present address: Department of Biochemistry, Brandeis University, Waltham, MA.

§ Department of Biochemistry & Biophysics.

⊥ Hormone Research Institute.

\* Abstract published in *Advance ACS Abstracts*, February 1, 1994.

<sup>1</sup> Abbreviations: AMC, 7-amino-4-methylcoumarin; tos-GPR-AMC, tosyl-Gly-Pro-Arg-AMC; tos-GPK-AMC, tosyl-Gly-Pro-Lys-AMC; Z-GPR-AMC, *N*-carbobenzoxy-L-Gly-Pro-Arg-AMC; Z-R-AMC, *N*-carbobenzoxy-L-Arg-AMC; Z-K-AMC, *N*-carbobenzoxy-L-Lys-AMC; MUGB, 4-methylumbelliferyl *p*-guanidinobenzoate; MUTMAC, 4-methylumbelliferyl *p*-(*N,N,N*-trimethylammonio)cinnamate chloride; BPTI, bovine pancreatic trypsin inhibitor; Z-GPR-SBzL, *N*-carbobenzoxy-Gly-Pro-Arg thiobenzyl ester; SBTI, soybean trypsin inhibitor.

to the Michaelis complex analog BPTI,<sup>1</sup> which contains Lys at the P1 site. We find that the S1 binding pocket, including the solvent structure, remains largely in a trypsin-like conformation. An acetate anion from the crystallization medium is present at the base of the specificity pocket, restoring a negative electrostatic potential to this region. Subsequent experiments demonstrated that exogenous acetate partially restores the activity of D189S toward substrates possessing Arg or Lys in the P1 position. These data provide a unique example of the functional replacement by a small molecule of an amino acid which is crucial to substrate binding, rather than directly to catalysis. The elucidation of the acetate binding site by crystallography also permits an analysis of the structural basis for rate enhancement, by means of a comparison with wild-type and mutant trypsins in which the negatively charged group is located in various positions in the pocket. The analysis shows that Asp189 plays a dual role in trypsin, providing both high substrate binding affinity as well as assistance in precise positioning of the scissile bond relative to the Ser195/His57 catalytic couple.

## MATERIALS AND METHODS

**Enzyme and Inhibitors.** Rat anionic trypsinogen D189S was expressed in yeast culture medium by fusing the trypsinogen coding sequence to the  $\alpha$ -factor leader peptide, as described (Phillips et al., 1990; Hedstrom et al., 1992). The zymogen form was purified by phenyl-Sepharose chromatography prior to activation by enterokinase treatment. The activated enzyme was further purified by affinity chromatography on SBTI Sepharose (Sigma Chemical Co.). BPTI for use in crystallization trials was purchased from Merck (Trasylol) and used without further purification. Chymotrypsin was purchased from Sigma. Purified anionic rat trypsin D189G was the generous gift of Christopher Tsu. All substrates were purchased from Bachem Biosciences, Inc.

**Crystallization.** Purified anionic rat trypsin D189S was exchanged into 1 mM HCl by Amicon filtration and stored at 4 °C at concentrations of 10–15 mg/mL. For crystallization, the enzyme was first adjusted to pH 7.0 by the addition of a small amount of concentrated Tris buffer. BPTI (stored at approximately 10 mg/mL in water) was mixed immediately with the concentrated enzyme at stoichiometries of 1:1 or a slight excess of inhibitor, and the complexes were incubated on ice for at least 1 h prior to setting up in crystallization trays. Crystals of the D189S–BPTI complex were obtained via hanging drop vapor diffusion against solutions containing 37% PEG 3350, 0.2 M ammonium acetate, and 0.1 M sodium citrate (pH 6.2) (final concentrations) at a temperature of 4 °C. The final concentration of the enzyme–inhibitor complex varied between 10 and 14 mg/mL.

**Structure Determination.** Crystals of rat trypsin D189S complexed with BPTI were stabilized in an artificial mother liquor containing 50% PEG 3350, 0.2 M ammonium acetate and 0.1 M sodium citrate (pH 6.2) for at least 12 h prior to mounting. Data collection was carried out on a Xentronics area detector, and the data were reduced using the XDS program package (Kabsch, 1988). Data from several crystals were used; the data were scaled together using the programs AGROVATA/ROTAVATA within the Cambridge (CCP4) crystallographic program package.

As the crystals are isomorphous with those of trypsin D189G/G226D complexed with C5A/C55A BPTI (Perona et al., 1993a), this trypsin complex was used as an initial model to provide phase information. The side chain of Asp226 was truncated to the wild-type Gly226; the side chain of Lys15

Table 1: Crystallographic Data for Rat Trypsin D189S Complexed with BPTI

space group	$P_{3}2_1$
cell dimensions (Å)	$a = 93.30$
	$c = 62.70$
$V_m$ (Å <sup>3</sup> /Da)	2.6
resolution (Å)	2.05
total obs	29466
unique obs	13004
% complete	68
$R_{\text{merge}}^a$ (%)	7.7
$R_{\text{cryst}}^b$ (%)	18.3 (6.0–2.05 Å)
rms bonds	0.011
rms angles (deg)	2.7

<sup>a</sup>  $R_{\text{merge}} = (\sum_h \sum_i |F_{hi}| - |F_{h\bar{i}}|) / (\sum_h |F_h|)$ , where  $\langle F_h \rangle$  is the mean structure factor amplitude of  $i$  observations of symmetry-related reflections with Bragg index  $h$ . <sup>b</sup>  $R_{\text{cryst}} = (\sum_h |F_{\text{obs}} - |F_{\text{calcd}}|) / (\sum_h |F_{\text{obs}}|)$ , where  $F_{\text{obs}}$  and  $F_{\text{calcd}}$  are the observed and calculated structure factor amplitudes, respectively.

of BPTI was truncated to Ala, and all solvent molecules were removed from the S1 binding pocket. Refinement was carried out using the program XPLOR (Brünger et al., 1987). Initial rigid-body refinement to exactly position the complex in the cell was followed by positional and individual  $B$  factor refinement. Refinement cycles were iterated with rebuilding of the model including the four N-terminal residues of BPTI, which (unlike the N-terminus of C5A/C55A BPTI complexed with D189G/G226D trypsin; Perona et al., 1993a) are well-ordered in this structure. Modeling was done using the INSIGHT (Dayringer et al., 1986; BIOSYM Corp., San Diego) and FRODO (Jones, 1985) molecular graphics programs implemented on an Evans & Sutherland PS390 graphics workstation. Crystallographic statistics are reported in Table 1. An OMIT map showing electron density in the region of the S1 binding pocket confirms the location of the acetate anion (Figure 1).

**Kinetic Evaluations.** The concentration of enzyme active sites was determined spectrofluorometrically using the chymotrypsin titrant MUTMAC for chymotrypsin, trypsin D189S, and trypsin D189G and the trypsin titrant MUGB for wild-type trypsin (Jameson et al., 1973). Fluorescence activity assays were performed by following the release of AMC from the amide substrates tos-GPR-AMC, tos-GPK-AMC, Z-GPR-AMC, Z-Arg-AMC, and Z-Lys-AMC as described (Higaki et al., 1989). Hydrolysis of the thiobenzyl ester substrate Z-GPR-SBzl was monitored at 324 nm by means of a coupled reaction with 4,4'-dithiobis(pyridine) (Craik et al., 1987). Assays carried out at pH 6.2 used 50 mM MES as the buffer species.

## RESULTS

**Structure of the Trypsin D189S–BPTI–Acetate Complex.** Substitution of Asp189 with Ser at the base of the S1 binding site occurs with little change in the position of backbone and side-chain atoms in the pocket when acetate is also bound. Interestingly, the interactions made by Lys15 of BPTI in this pocket are identical in trypsin D189S and in wild-type bovine trypsin (the specificity pockets of rat and bovine trypsin are identical, as judged by comparison of the structures of each enzyme complexed with benzamidine; Krieger et al., 1974; M. E. McGrath and R. J. Fletterick, unpublished results). In each case, the  $\text{N}\epsilon$  group of the lysine lies within hydrogen-bonding distance of the side-chain hydroxyl group of Ser190, the main-chain carbonyl oxygen of this residue, and two water molecules (WATS 1 and 3, Figure 2). The positions of these two waters are also unchanged in the mutant enzyme.

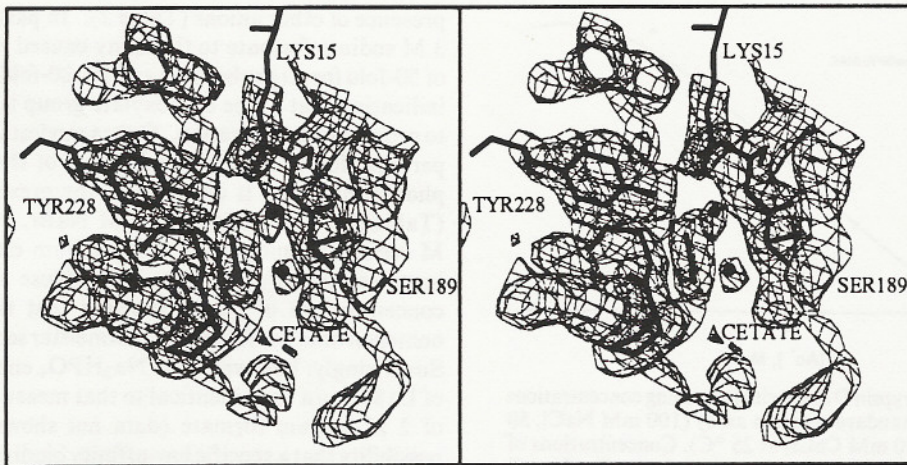


FIGURE 1: Stereoview of part of a  $2F_0 - F_c$  residue omit map, in the region of the primary binding pocket, contoured at  $1.2\sigma$ . Atoms shown were deleted from the structure, and refinement was carried out with these atoms omitted, prior to calculation of the map. Phases and calculated amplitudes for the map calculation were then obtained from a structural model with these atoms omitted. Dark circles in the foreground represent water molecules.

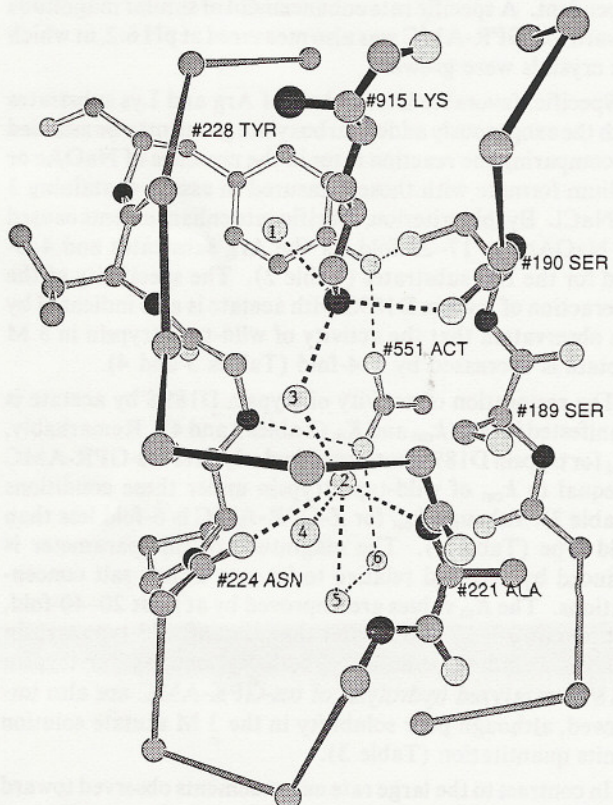


FIGURE 2: Polar interactions in the S1 site of trypsin D189S. An  $\alpha$ -carbon trace of the three  $\beta$ -strands forming the pocket together with two connecting loops (bottom) is depicted. Nitrogen atoms are shown in dark gray, carbons are intermediate in shading, and oxygens appear in light gray. Larger circles indicate that the atoms occupy positions farther in the foreground. The lysine side chain of BPTI, which binds in the S1 site, is shown at the top (#915 LYS). The acetate moiety (#551 ACT) is at center. Unconnected circles represent water molecules 1–6. Hydrogen-bonding interactions are indicated by dashed lines. Nomenclature for the substrate amino acid residues is ( $P_n, \dots, P_2, P_1, P_1', P_2', \dots, P_n'$ ) where  $P_1-P_1'$  denotes the hydrolyzed bond. ( $S_n, \dots, S_2, S_1, S_1', S_2', \dots, S_n'$ ) denote the corresponding enzyme binding sites (Schechter & Berger, 1968).

Interactions of the reactive loop of BPTI with the oxyanion hole of trypsin D189S at positions 193–195, as well as with the Ser195 side chain, are identical to those seen in the structure of rat trypsin D189G/G226D complexed with BPTI (Perona et al., 1993a). Antiparallel  $\beta$ -sheet hydrogen bonding at positions Ser214–Gly216 of the enzyme, as well as the

interactions made with several more distal enzyme surface loops, is also unchanged.

The side-chain hydroxyl group of Ser189 is oriented outside of the binding pocket (Figures 2 and 4). While the hydroxyl group of this residue is located within hydrogen-bonding distance of the backbone amide nitrogen of Ala221, the relative orientation of the two groups indicates that the interaction has no substantial hydrogen-bonding character. No other polar interactions stabilize the orientation of the Ser189 side chain. No significant alteration in the positions or relative thermal factors of nearby enzyme groups, when compared to the structures of trypsin D189G/G226D or wild-type bovine trypsin, was detected. However, the solvent structure in the pocket is modified due to the presence of the acetate ion (see below).

*Interactions of the Acetate Ion.* An acetate ion is located at the base of the specificity pocket and is oriented such that its carboxylate group projects in the direction of Lys15 of BPTI (Figure 2). It is well-ordered, as indicated by an average B factor for the four atoms of  $25 \text{ \AA}^2$ . Several observations confirm that the electron density corresponds to acetate rather than several water molecules. First, all attempts at fitting the electron density with waters resulted in the appearance of large residual peaks in electron density maps computed from coefficients ( $F_0 - F_c$ ). Further, the electron density in maps computed from coefficients ( $2F_0 - F_c$ ) during these iterations consistently appeared as flat and triangular, suggesting the presence of acetate. Finally, refinement carried out after the inclusion of acetate in the structural model resulted in ( $F_0 - F_c$ ) difference electron density maps which were essentially featureless in this region.

The methyl group of the acetate is located between, and approximately  $3.6 \text{ \AA}$  distant from, polypeptide backbone atoms at positions 189–190 and 183–184. Side-chain atoms of Ile138 and Leu158 lie directly beneath the acetate methyl group at distances of  $3.8$ – $4.0 \text{ \AA}$ . As has been noted previously (Perona et al., 1993a), this region of the trypsin hydrophobic core adjacent to the binding pocket is very poorly packed. Removal of the Asp189 group and placement of the Ser189 hydroxyl group outside of the pocket allow access to this region through the primary binding pocket. The acetate methyl group is oriented toward the hydrophobic core but does not significantly fill the void space resulting from the poor packing. Binding of acetate at this position displaces a water molecule that

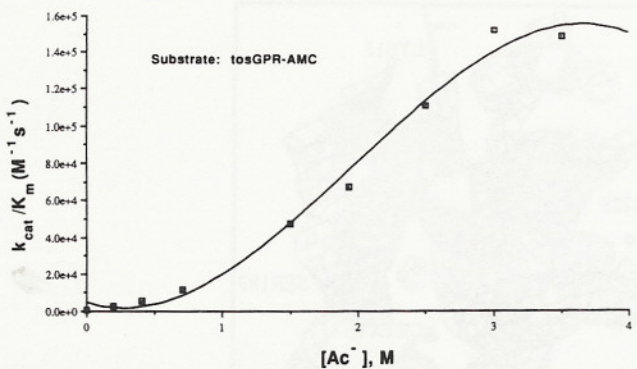


FIGURE 3: Activation of trypsin D189S with increasing concentrations of NaOAc added to the standard reaction assay (100 mM NaCl, 50 mM Tris (pH 8.0), and 20 mM CaCl<sub>2</sub> at 25 °C). Concentrations of the substrate tos-GPR-AMC were chosen to be <<K<sub>m</sub> for all measurements. Under these conditions  $v = (k_{cat}/K_m)[E_o][S]$  (Fersht, 1985). Data represent the average of at least three kinetic runs.

bridges the side chains of Asp189 and Tyr228 in wild-type trypsin.

The carboxylate group of the acetate makes numerous polar interactions with enzyme moieties, as well as water molecules located in the S1 binding pocket (Figure 2). One carboxylate oxygen accepts a hydrogen bond from the phenolic hydroxyl of Tyr228, the other from the backbone amide group at position Gly226. The latter oxygen also forms hydrogen bonds with two waters. One of these (WAT2, Figure 2) appears to play an important role in stabilizing the orientation of the acetate, as it also interacts strongly with backbone groups at positions Ala221 and Asn224. Further, this water hydrogen-bonds with WAT3 (Figure 2), which bridges to the positively charged Nε of Lys15 of the BPTI inhibitor. Thus, although one oxygen of the acetate carboxylate is located just 4.1 Å from the positively charged amine of Lys15 of BPTI, the interaction between these two oppositely charged groups is mediated through two rather than one water molecule.

Because the side chain of Ser189 makes no favorable interactions in its observed orientation, it is reasonable to suggest that it may adopt an alternative conformation in the absence of acetate. Indeed, modeling the Ser189 Oγ hydroxyl in the position occupied by Cγ of Asp189 results in a steric clash with both the acetate as well as the new water, WAT2. Therefore, occupancy of the S1 site by acetate and WAT2 very likely drives the rotation of Ser189 away from this pocket. In the absence of these ligands, other waters in the region would adopt alternate positions, possibly providing favorable interactions for the Ser189 hydroxyl group. Of the remaining waters in the immediate vicinity, WAT4 occupies the same position as in the wild-type bovine trypsin pocket when BPTI is bound, and WAT5 and WAT6 are displaced by 0.6–0.8 Å (Figure 2).

**Activation of Trypsin D189S by NaOAc.** Addition of sodium acetate enhances the activity of trypsin D189S (Tables 2–4, Figure 3). The activity increases with increasing amounts of NaOAc and does not exhibit apparent saturation until a concentration of 3 M is reached (Figure 3), indicating a very weak free energy of interaction. Nonetheless, in the presence of 3 M NaOAc, trypsin D189S-catalyzed hydrolysis of single-residue and tripeptide amide substrates possessing Arg in the P1 position increases by 250–300-fold (Table 2). In contrast, trypsin D189S hydrolyzes substrates containing Lys in the P1 position only 20–40-fold more rapidly in the presence of 3 M NaOAc (Tables 2 and 3).

While the increase in activity of trypsin D189S is greatest when acetate is bound, modest activation also occurs in the

presence of other anions (Table 2). In particular, addition of 3 M sodium formate to the assay caused rate enhancements of 50-fold for Arg substrates and 10–20-fold for Lys substrates, indicating that a free carboxylate group is in itself sufficient to provide some activation. Only a modest increase in activity, perhaps due to a “salting-in” effect of the relatively hydrophobic substrate, is observed in the presence of 3 M NaCl (Table 2). The addition of 3 M NaBr, 3 M (NH<sub>4</sub>)<sub>2</sub>SO<sub>4</sub>, 3 M sodium propionate, or 2 M sodium citrate caused small increases equal to or less than those observed at these concentrations of NaCl, showing that the activation phenomenon does not follow the Hofmeister series (Jencks, 1969). Surprisingly, however, 2 M Na<sub>2</sub>HPO<sub>4</sub> enhanced the activity of D189S to a level identical to that measured in the presence of 2 M sodium formate (data not shown), suggesting the possibility that a specific low-affinity binding site for phosphate may exist at the base of the S1 site of trypsin D189S as well. The rate enhancement measured in the presence of 3 M KOAc and 3 M NH<sub>4</sub>OAc is identical to that provided by 3 M NaOAc (data not shown), showing that the phenomenon is not cation-dependent. A specific rate enhancement of similar magnitude toward tos-GPR-AMC was also measured at pH 6.2, at which the crystals were grown.

Specific, favorable interactions of Arg and Lys substrates with the exogenously added carboxylate group may be assessed by comparing the reaction rates in the presence of NaOAc or sodium formate with those measured in assays containing 3 M NaCl. By this criterion, specific rate enhancements caused by NaOAc are 17–23-fold for the Arg substrates and 4–6-fold for the Lys substrates (Table 2). The specificity of the interaction of trypsin D189S with acetate is also indicated by the observation that the activity of wild-type trypsin in 3 M acetate is decreased by 2–4-fold (Tables 3 and 4).

The restoration of activity of trypsin D189S by acetate is manifested in both  $k_{cat}$  and  $K_m$  (Tables 3 and 4). Remarkably,  $k_{cat}$  for trypsin D189S-catalyzed hydrolysis of tos-GPR-AMC is equal to  $k_{cat}$  of wild-type trypsin under these conditions (Table 3), although  $k_{cat}$  for Z-GPR-AMC is 6-fold less than wild type (Table 4). The magnitude of this parameter is reduced by 2–3-fold relative to its rate at low salt concentrations. The  $K_m$  values are improved by at least 20–40-fold, but remain 10–30-fold greater than that of wild-type trypsin (Tables 3 and 4). Similarly, both  $k_{cat}$  and  $K_m$  for trypsin D189S-catalyzed hydrolysis of tos-GPK-AMC are also improved, although poor solubility in the 3 M acetate solution limits quantitation (Table 3).

In contrast to the large rate enhancements observed toward tos-GPR-AMC and Z-GPR-AMC,  $k_{cat}/K_m$  for esterolysis of Z-GPR-SBzl by trypsin D189S is increased by only 4–5-fold in the presence of 3 M NaCl, 3 M sodium formate, or 3 M NaOAc (Tables 2 and 4). Therefore, no specific effect of the exogenous carboxylate group exists for the acceleration of ester hydrolysis. In the presence of chloride, formate, or acetate, trypsin D189S hydrolyzes the ester substrate as efficiently as wild-type trypsin. Only a small rate enhancement is observed because trypsin D189S is already an efficient, nonspecific esterase (Hedstrom et al., 1992). The  $k_{cat}$  of trypsin and trypsin D189S for esterolysis is decreased 5–10-fold in 3 M NaOAc, while  $K_m$  is improved by 25-fold for trypsin D189S (Table 4).

Mechanistic kinetic parameters for amide hydrolysis by trypsin can be derived from an analysis of steady-state kinetic data measured toward equivalent ester and amide substrates (Table 5; Zerner et al., 1964). Since  $k_{cat(amide)}$  is approximately equal to  $k_{cat(ester)}$  for trypsin, in either the presence or absence

Table 2: Rate Enhancement of Trypsin D189S toward Amide and Ester Substrates<sup>a</sup>

substrate	standard assay	$k_{cat}/K_m (\text{M}^{-1} \text{s}^{-1})$		
		+3 M NaCl	+3 M sodium formate	+3 M NaAc
tos-GPR-AMC	515 ± 13	6670 ± 170 [12.9]	(2.8 ± 0.2) × 10 <sup>4</sup> [53.7]	(1.5 ± 0.1) × 10 <sup>5</sup> [295]
tos-GPK-AMC	182 ± 3	1180 ± 117 [6.5]	3500 ± 170 [19.2]	7170 ± 1670 [39.5]
Z-R-AMC	0.29 ± 0.01	4.1 ± 0.2 [14.1]	12.5 ± 0.3 [43.6]	70.3 ± 2.5 [242]
Z-K-AMC	0.12 ± 0.003	0.74 ± 0.08 [6.2]	1.4 ± 0.1 [11.8]	2.6 ± 0.2 [21.7]
Z-GPR-SBzl	(1.63 ± 0.05) × 10 <sup>5</sup>	(6.0 ± 0.4) × 10 <sup>5</sup> [3.7]	(8.8 ± 0.6) × 10 <sup>5</sup> [5.4]	(7.2 ± 0.3) × 10 <sup>5</sup> [4.4]

<sup>a</sup> Hydrolysis of single-residue and tripeptide substrates by trypsin D189S. Standard assay conditions are 50 mM Tris (pH 8.0), 100 mM NaCl, and 20 mM CaCl<sub>2</sub> at 25 °C. Assay buffers containing 3 M NaCl, 3 M sodium formate, and 3 M NaOAc were adjusted to pH 8.0. Substrate concentrations were <<K<sub>m</sub>. Data were analyzed by linear regression; the average and standard deviation of at least three kinetic runs are reported. Numerals in brackets refer to the rate enhancement relative to the standard assay conditions, determined as the ratio of  $k_{cat}/K_m$  values.

Table 3: Kinetic Parameters for Reconstitution of Trypsin D189S by Exogenous Acetate<sup>a</sup>

enzyme	$k_{cat} (\text{s}^{-1})$	$K_m (\mu\text{M})$	$k_{cat}/K_m (\text{M}^{-1} \text{s}^{-1})$
tos-GPR-AMC, standard assay			
trypsin	61.3 ± 0.7	3.7 ± 0.1	(1.65 ± 0.008) × 10 <sup>7</sup>
trypsin D189S	1.2 ± 0.5	2200 ± 900	515 ± 13
tos-GPR-AMC, 3 M NaAc			
trypsin	20 ± 0.7	4.3 ± 0.1	(4.67 ± 0.33) × 10 <sup>6</sup>
trypsin D189S	18.3 ± 6.7	120 ± 60	(1.5 ± 0.17) × 10 <sup>5</sup>
tos-GPK-AMC, standard assay			
trypsin	43.3 ± 6.7	16 ± 1.6	(2.83 ± 0.17) × 10 <sup>6</sup>
trypsin D189S	>0.45 <sup>b</sup>	>2500	182 ± 3
tos-GPK-AMC, 3 M NaAc			
trypsin	25 ± 3.3	19 ± 4.7	(1.3 ± 0.15) × 10 <sup>6</sup>
trypsin D189S	>2.2 <sup>c</sup>	>310	6670 ± 1670

<sup>a</sup> Steady-state kinetic constants for trypsin and trypsin D189S under standard conditions and upon activation by 3 M NaOAc. Standard conditions are as described in Table 2. The average and standard deviation of at least two kinetic runs are reported. <sup>b</sup> No saturation was observed at 500 μM substrate. <sup>c</sup> No saturation was observed at 62 μM substrate.

of 3 M NaOAc, and for trypsin D189S in the presence of 3 M NaOAc (Table 4), it is likely that deacylation is the rate-determining step for these reactions (see Discussion). It is not possible to establish definitively the rate-determining step for trypsin D189S-catalyzed hydrolysis of Z-GPR-AMC in the absence of acetate, owing to the lack of substrate saturation. However, comparison of the hydrolysis of tos-GPR-AMC and Z-GPR-AMC by trypsin D189S and other variants (Tables 3 and 4; C. Tsu and C. S. Craik, unpublished results) has shown that K<sub>m</sub> values for tos-GPR-AMC are invariably 2–10-fold lower than those for Z-GPR-AMC, whereas k<sub>cat</sub> values are no more than 2-fold lower. Therefore, it is highly likely that k<sub>cat</sub> for trypsin D189S toward Z-GPR-AMC remains considerably lower than toward Z-GPR-SBzl (Table 4), which would indicate that acylation is the rate-limiting step in this reaction.

Since the Ser189 side chain of trypsin D189S makes no specific interactions with the acetate anion, it might be expected that other trypsin variants lacking the Asp189 carboxylate would also manifest a rate enhancement in the presence of this ligand. To test this proposal, the k<sub>cat</sub>/K<sub>m</sub> values for trypsin D189G were measured toward the tos-GPR-AMC and tos-GPK-AMC substrates in standard assay buffer, as well as in the presence of 3 M NaCl and of 3 M NaOAc. This mutant also exhibited specific rate enhancements toward both substrates in the presence of acetate, although the maximum

Table 4: Hydrolysis of Peptidyl Ester and Amide Substrates by Trypsin and Trypsin D189S<sup>a</sup>

enzyme	$k_{cat} (\text{s}^{-1})$	$K_m (\mu\text{M})$	$k_{cat}/K_m (\text{M}^{-1} \text{s}^{-1})$
Z-GPR-AMC, standard assay			
trypsin	77 ± 0.5	20.7 ± 0.3	(3.72 ± 0.05) × 10 <sup>6</sup>
trypsin D189S	>1.1 <sup>b</sup>	>10000	112 ± 1.7
Z-GPR-AMC, 3 M NaAc			
trypsin	49.2 ± 7.7	29 ± 5	(1.68 ± 0.03) × 10 <sup>6</sup>
trypsin D189S	8.3 ± 5.8	260 ± 200	(3.3 ± 0.3) × 10 <sup>4</sup>
Z-GPR-SBzl, standard assay			
trypsin	101.5 ± 3.0	30 ± 3.5	(3.53 ± 0.28) × 10 <sup>6</sup>
trypsin D189S	41.6 ± 1.4	310 ± 25	(1.35 ± 0.07) × 10 <sup>5</sup>
Z-GPR-SBzl, 3 M NaAc			
trypsin	10.2 ± 1.3	18 ± 8	(5.83 ± 1.7) × 10 <sup>5</sup>
trypsin D189S	20.9 ± 4.1	32 ± 8	(6.54 ± 0.44) × 10 <sup>5</sup>

<sup>a</sup> Steady-state kinetic constants for trypsin and trypsin D189S toward the equivalent amide and ester substrates Z-GPR-AMC and Z-GPR-SBzl, respectively. Standard conditions are as described in Table 2. Esterolysis reactions were carried out in the presence of 250 μM 4,4'-dithiobis(pyridine), which reacts with the thiobenzyl leaving group to produce a compound with absorbance at 324 nm. The average and standard deviation of at least two kinetic runs are reported. <sup>b</sup> No saturation was observed at 2 mM substrate.

velocity toward the Arg substrate was decreased approximately 5-fold relative to trypsin D189S (data not shown).

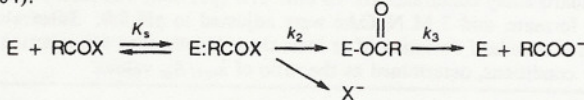
## DISCUSSION

**Structural Basis for the Activation of Trypsin D189S by Acetate.** The crystal structure of trypsin D189S complexed with BPTI and acetate provides a structural basis for understanding the acceleration of D189S-catalyzed amide hydrolysis by acetate. The hydrophobic interactions made by the methyl group of acetate clearly play an important role in this activation, as is demonstrated by the observation that activation by formate is significantly less effective (Table 2). Most probably, the hydrophobic interactions of the methyl group are important to stable positioning of the carboxylate in an orientation where it can interact with substrate. Alternatively, the lower rate enhancement measured in 3 M sodium formate may reflect an absence of saturation for this weaker binding ligand. The absence of a specific enhancement by propionate suggests that the additional methyl group of this anion cannot be accommodated in the S1 site. Propionate cannot bind in the same orientation as acetate, owing to the fact that the acetate methyl group is relatively closely surrounded by the Ile138 and Leu158 side chains. The

Table 5: Mechanistic Kinetic Parameters for Hydrolysis of Z-GPR-AMC and Z-K-AMC by Trypsin, Trypsin D189S, and Trypsin D189G/G226D<sup>a</sup>

	Z-GPR-AMC			Z-K-AMC		
	$K_s$ ( $\mu\text{M}$ )	$k_2$ ( $\text{s}^{-1}$ )	$k_3$ ( $\text{s}^{-1}$ )	$K_s$ ( $\mu\text{M}$ )	$k_2$ ( $\text{s}^{-1}$ )	$k_3$ ( $\text{s}^{-1}$ )
trypsin	86	319	101.5	170	0.47	112
trypsin D189S	>10000 <sup>b</sup>	>1.1	126.2			
trypsin D189G/G226D <sup>c</sup>	290	0.033	150	1500	0.007	52

<sup>a</sup> Values of the binding constant  $K_s$ , acylation rate constant  $k_2$ , and deacylation rate constant  $k_3$  under standard assay conditions. Values for D189S were computed from the steady-state kinetic constants of Table 4, according to the standard serine protease mechanism (Zerner et al., 1964):



For reactions in which acylation is the rate-determining step,  $K_m = K_s$  and  $k_{cat} = k_2$ . If deacylation is rate-determining, then  $K_m = K_s [k_{cat,ester}/(k_2 + k_{cat,ester})]$  and  $k_{cat} = k_2 k_{cat,ester}/(k_2 + k_{cat,ester})$ . <sup>b</sup> No saturation is observed at 2 mM substrate. <sup>c</sup> Parameters are calculated from data in Perona et al. (1993b) and from unpublished observations (C. Tsu and C. S. Craik).

observation that exogenous phosphate causes a rate enhancement similar to that formate suggests the possibility that this anion can also be bound specifically. Interestingly, the similar sulfate anion fails to exhibit any specific activation.

While a considerable rate enhancement is achieved by the addition of acetate, it is nonetheless clear that its interactions with substrate are nonoptimal. The anchoring of the methyl group orients one oxygen of the acetate carboxylate toward the base of the S1 binding pocket into a network of water molecules (Figure 2). The waters are likely to dissipate a portion of the negative charge on the carboxylate, thereby decreasing the free energy available for binding to the positively charged substrate. Thus, even at saturating concentrations of acetate,  $k_{cat}/K_m$  is only 3% of that exhibited by wild-type trypsin under these conditions (Table 3).

The position of the acetate in the S1 binding pocket of trypsin D189S illustrates the rationale for conservation of the negative charge at position 189 to maximize the free energy of binding. At this position, both oxygens of the carboxylate are easily oriented toward substrate and make no strong interactions with other enzyme groups (Ruhlmann et al., 1973; Krieger et al., 1974). Reductions in substrate binding efficiency toward amide substrates possessing Arg and Lys at position P1 were measured for trypsin D189G/G226D, where the Asp226 carboxylate was observed to be partially sequestered from substrate by interactions with other enzyme groups (Perona et al., 1993b). Therefore, both variants are compromised in catalytic efficiency because the position of the negatively charged binding determinant is nonoptimal (Figure 4). The observation that trypsin D189G is also activated by acetate suggests that the phenomenon may be general for trypsin variants which lack an Asp or Glu residue at the base of the binding pocket, provided that accessibility to the methyl group binding site is retained.

Rate enhancement in the presence of saturating concentrations of acetate is substantially greater for Arg relative to Lys substrates (Tables 2 and 3). To assess the interactions that Arg is likely to make in the S1 pocket of trypsin D189S, a model was constructed by superimposing the structure of trypsin D189G/G226D complexed with the BPTI analog APPI (Perona et al., 1993a), which possesses an Arg as the P1 site residue. The modeling suggests that one terminal nitrogen of the Arg guanidinium group makes a single ionic

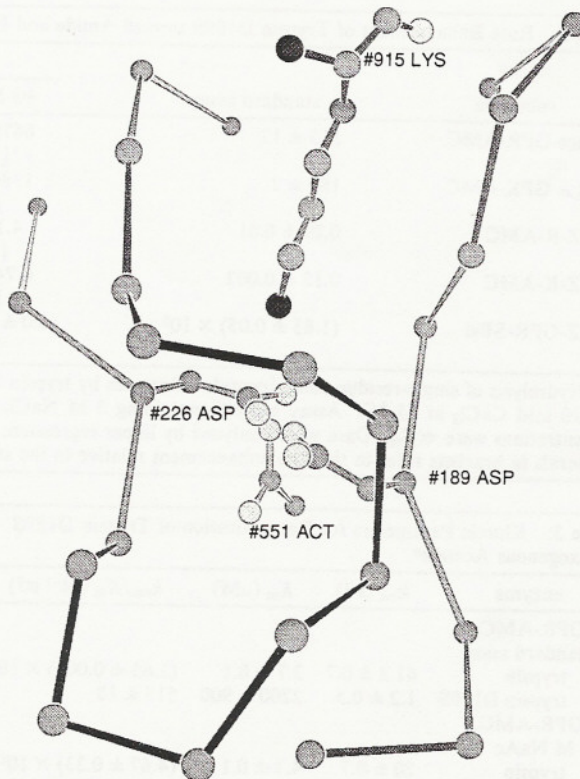
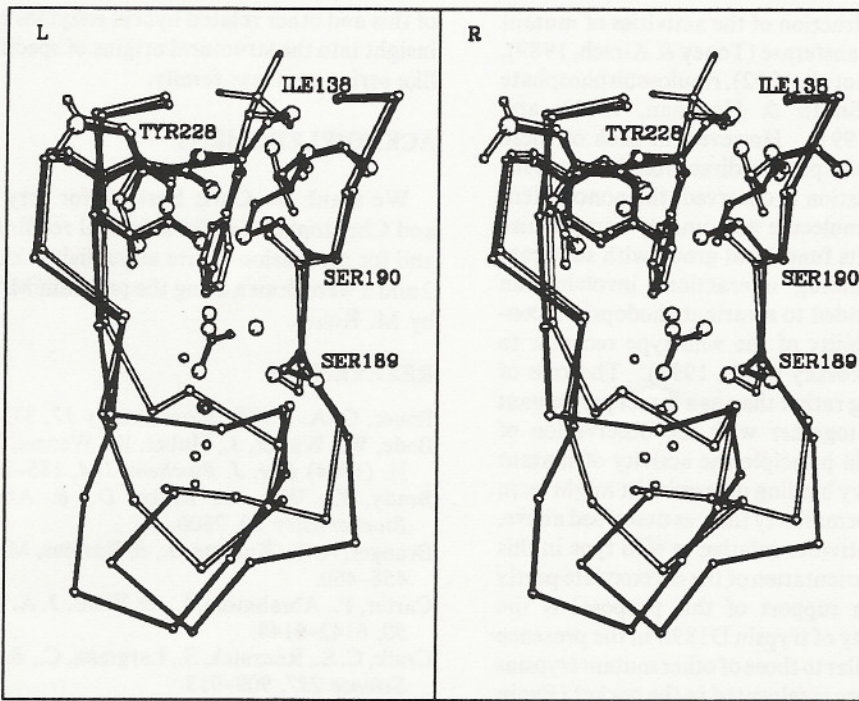


FIGURE 4: Comparisons of the positions of the negatively charged carboxyl group in the primary binding pocket of trypsin, trypsin D189G/G226D, and trypsin D189S with acetate bound. The  $\alpha$ -carbon trace and position of the lysine side chain of BPTI, which binds in the S1 site, are derived from the structure of trypsin D189S complexed with BPTI. The positions of Asp226 and Asp189 were taken from the crystal structures of trypsins D189G/G226D (Perona et al., 1993b) and wild-type rat trypsin (M. E. McGrath, unpublished results), respectively, after superposition of each on the structure of trypsin D189S.

interaction with one carboxylate oxygen of the acetate. This oxygen is well-positioned to interact with the Arg substrate, as its only polar interaction within the pocket is as a hydrogen-bond acceptor from the hydroxyl group of Tyr228 in an orientation that is *anti* with respect to the orbitals of the carboxylate (Figure 2).

The low solubility of substrates at 3 M NaOAc precludes the precise quantitation of Lys substrate kinetic parameters (Table 3). Therefore, the rationale for the 10-fold greater activation by acetate of Arg relative to Lys substrate cleavage is not immediately apparent from this analysis. It is of interest, nevertheless, to consider the fact that the interaction of Lys15 of BPTI with acetate in trypsin D189S is mediated by two water molecules (Figure 2). A detailed kinetic and crystallographic analysis of trypsin D189G/G226D suggested that direct ionic contacts in the trypsin S1 site do not significantly improve the free energy of substrate binding relative to water-mediated interactions (Perona et al., 1993a). However, the mediation of the electrostatic interaction between enzyme and substrate for wild-type trypsin and trypsin D189G/G226D occurs through a single water. Mediation by two waters could cause the free energy gain potentially realizable from charge neutralization to be dissipated by the other hydrogen-bonding interactions made by the waters (Figure 2). Less free energy of binding of Lys substrates would then be available for translation into a high catalytic rate. The crystal structure of trypsin D189S complexed with APPI, together with the determination of  $K_s$  values for both Arg and Lys substrate catalysis at 3 M NaOAc by pre-steady-state kinetic analysis (see below), will provide further information to test this model.



**FIGURE 5:** Superposition of  $\alpha$ -carbon traces of the primary S1 binding pockets of chymotrypsin and of rat trypsin D189S.  $\gamma$ -Chymotrypsin is visualized in a complex with N-acetyl-L-leucyl-L-phenylalanyl trifluoromethyl ketone (PDB 7GCH) (Brady et al., 1990). Solid lines represent trypsin and open lines represent chymotrypsin. Labels refer to side chains in trypsin. Waters present in the trypsin pocket are shown as smaller circles; larger circles represent waters in the pocket of chymotrypsin. The acetate ligand bound to the pocket of trypsin D189S is shown at center. In D189S, orientation of Ser189 out of the pocket and binding of the side chain of Lys15 of BPTI inside the pocket may be consequences of the presence of bound acetate. The crystal structure of chymotrypsin complexed with BPTI shows that Lys15 is oriented out of the binding pocket where it interacts with the carbonyl group of Ser217 (Dr. T. Hynes, personal communication).

**A Dual Role for Asp189.** Efficient catalysis by serine proteases depends upon optimal alignment of the substrate scissile bond with the catalytic Ser195 and His57 side chains. A precise alignment results in a high value for the acylation rate constant  $k_2$ , as this constant reflects both the rate of nucleophilic attack by the Ser195 O $\gamma$  on the substrate carbonyl carbon, as well as the rate of expulsion of the leaving group. For variants such as trypsins D189S and D189G/G226D in which the catalytic machinery is intact, decreases in  $k_2$  very likely represent a misalignment of the scissile bond with these enzyme groups. The observation that the structure of the catalytic triad in these mutants is identical to that of wild-type trypsin supports this proposal (Perona et al., 1993b). Determination of  $k_2$  for amide hydrolysis by these trypsin variants (Table 5, footnotes) thereby permits evaluation of the role of the carboxylate group at the base of the S1 site in facilitating optimal substrate alignment.

As discussed above, it is highly likely that acylation is rate-determining for trypsin D189S-catalyzed hydrolysis of Z-GPR-AMC in the absence of acetate. Therefore, the values of  $K_s$  and  $k_2$  for this reaction are not substantially higher than the lower bounds indicated (Table 5).  $k_2$  for D189S-catalyzed hydrolysis of Z-GPR-AMC therefore remains considerably lower than that for wild-type trypsin. This result indicates that the distal ionic interactions between the P1 substrate side chain and Asp189 do contribute to precise positioning of the substrate scissile bond relative to the catalytic machinery. Since the substrate binding affinity in the absence of acetate is also substantially weakened for D189S (Table 5), we conclude that Asp189 plays a dual role in providing both substrate binding affinity as well as accurate positioning of the substrate scissile bond.

The  $k_{cat}$  values measured for trypsin-catalyzed hydrolysis of Z-GPR-AMC and Z-GPR-SBzl in the presence of 3 M NaOAc show that the turnover number for the amide substrate

is 5-fold higher than that for the equivalent ester (Table 4), precluding estimation of  $K_s$ ,  $k_2$ , and  $k_3$  for this reaction. One possible explanation for this observation is that the rate of leaving-group dissociation for the thiobenzyl ester substrate is decreased under conditions of very high ionic strength. Estimates of  $K_s$ ,  $k_2$ , and  $k_3$  for the D189S-catalyzed hydrolysis of Z-GPR-AMC at 3 M NaOAc from these steady-state measurements may also be unreliable. However, analysis of mechanistic kinetic parameters for hydrolysis of Lys- and Arg-containing amide substrates by trypsin D189G/G226D shows that relocation of the negative charge to Asp226 causes  $k_2$  to decrease and  $K_s$  to increase for both Lys and Arg substrate catalysis (Table 5). These results indicate that both binding affinity and substrate positioning are compromised by a nonoptimal placement of the carboxylate group and provide further evidence that this moiety plays a dual role. However, it is important to note that in the case of trypsin D189G/G226D, as well as in other variants (Evnin et al., 1990), the negatively charged carboxylate was repositioned closer to the catalytic machinery. Therefore, each of these variants is likely to possess a smaller S1 site, leading to steric hindrance for the large Arg side chain and consequent mispositioning on this basis. The position of acetate in trypsin D189S is deeper in the S1 site than is the carboxylate of Asp189 (Figure 4), permitting an unbiased evaluation of the role of its position in its ability to aid in the alignment of Arg substrates. Therefore, determination of  $K_s$ ,  $k_2$ , and  $k_3$  for the D189S-catalyzed hydrolysis of Z-GPR-AMC at 3 M NaOAc by pre-steady-state kinetic analysis will be valuable in further assessing the role of the position of the carboxylate group on the precise alignment of the scissile bond.

It is of interest to consider whether the noncovalent nature of the interaction between acetate and enzyme could itself be partly responsible for the diminished activities relative to wild-type trypsin. Chemical rescue by exogenous small molecules

reconstitutes only a small fraction of the activities of mutant forms of aspartate aminotransferase (Toney & Kirsch, 1989), carboxypeptidase (Phillips et al., 1992), ribulosebisphosphate carboxylase/oxygenase (Smith & Hartman, 1991), and subtilisin (Carter et al., 1991). However, in each of these examples the small molecule plays a direct role in catalysis. Even in cases where saturation is observed, the noncovalent interactions of the small molecule presumably compromise the precise orientation of its functional group with substrate moieties. Conversely, binding interactions involving an exogenous *n*-alkylamine added to a variant rhodopsin reconstituted 30–40% of the ability of the wild-type receptor to activate transducin (Zhukovsky et al., 1991). The role of acetate in substrate binding rather than as a direct participant in the catalytic process, together with the observation of saturation, suggests that in principle the activity of mutant trypsins lacking the primary binding determinant might be in great part restorable. It seems likely that, as described above, the 30–50-fold reduced activities relative to wild type in this case are mainly due to the orientation of the carboxylate partly away from substrate. In support of this proposal is the observation that the activity of trypsin D189S in the presence of saturating acetate is similar to those of other mutant trypsins in which the negative charge is relocated in the pocket (Evnin et al., 1990; Perona et al., 1993a,b). Complete activation even in the event of a properly oriented exogenously added carboxylate would be unlikely, however, because of the necessary entropic cost associated with ordering the small-molecule ligand.

**Conversion of Trypsin to Chymotrypsin.** The crystal structure of trypsin D189S provides information of importance to understanding the divergent P1-site specificities of trypsin and chymotrypsin. Since no structural changes beyond the positioning of nearby water molecules are observed between trypsin and trypsin D189S, all of the other differences between the S1 sites of trypsin and chymotrypsin are still present in the variant (Figure 5). These differences encompass the remaining solvent structure at the base of the S1 site, the orientation and identity of amino acid side chains at positions 138, 190 and 192, and the altered backbone conformation at residues 216–219 on the lip of the pocket. As D189S fails to exhibit a significant improvement in hydrolysis of P1-Phe-containing amide substrates relative to trypsin (Hedstrom et al., 1992), the crystal structure of this mutant therefore shows that these differences must be of critical importance to determining chymotryptic specificity. The lack of structural perturbation also suggests that the decreased activity toward basic residues is due solely to the removal of the negative charge. However, a further rationale for the decreased activities could be that the pocket may be partially disordered in the absence of either substrate or acetate, as is suggested by a diminished affinity of proflavin binding (Hedstrom et al., submitted for publication).

The substrate specificities of trypsin and chymotrypsin are profoundly influenced by surrounding amino acids (Hedstrom et al., 1992; Hedstrom et al., submitted for publication; Perona et al., submitted for publication). While introduction of the substitutions I138T/Q192M/T218 fails to transfer chymotryptic specificity to trypsin, this property is endowed by the further exchange of two adjacent surface loops (Figure 5, bottom). Detailed functional and structural characterization

of this and other related hybrid enzymes provides substantial insight into the structural origins of specificity in the trypsin-like serine protease family.

## ACKNOWLEDGMENT

We thank Dr. Chris Bystroff for very helpful discussions and Christopher Tsu for a critical reading of the manuscript and for permission to cite unpublished kinetic data. Figures 2 and 4 were drawn using the program MAXIMAGE written by M. Rould.

## REFERENCES

- Bauer, C.-A. (1978) *Biochemistry* 17, 375–380.
- Bode, W., Walter, J., Huber, R., Wenzel, H. R., & Tschesche, H. (1984) *Eur. J. Biochem.* 144, 185–190.
- Brady, K., Wei, A., Ringe, D., & Abeles, R. H. (1990) *Biochemistry* 29, 7600.
- Brunger, A. T., Kuriyan, J., & Karplus, M. (1987) *Science* 235, 458–460.
- Carter, P., Abrahmsen, L., & Wells, J. A. (1991) *Biochemistry* 30, 6142–6148.
- Craik, C. S., Rocznak, S., Largman, C., & Rutter, W. J. (1987) *Science* 237, 909–913.
- Dayringer, H., Tramontano, A., Sprang, S., & Fletterick, R. J. (1986) *J. Mol. Graphics* 4, 82–91.
- Evnin, L. B., Vasquez, J. R., & Craik, C. S. (1990) *Proc. Natl. Acad. Sci. U.S.A.* 87, 6659–6663.
- Fersht, A. R. (1985) *Enzyme Structure and Mechanism*, 2nd ed., Freeman, New York.
- Graf, L., Jancso, A., Szilagyi, L., Hegyi, G., Pinter, K., Naray-Szabo, G., Hepp, J., Medzihradszky, K., & Rutter, W. J. (1988) *Proc. Natl. Acad. Sci. U.S.A.* 85, 4961–4965.
- Hedstrom, L., Szilagyi, L., & Rutter, W. J. (1992) *Science* 255, 1249–1253.
- Higaki, J. N., Evnin, L. B., & Craik, C. S. (1989) *Biochemistry* 28, 9256–9263.
- Jameson, G. W., Roberts, D. V., Adams, R. W., Kyle, W. S. A., & Elmore, D. T. (1973) *Biochem. J.* 131, 107–117.
- Jencks, W. P. (1969) *Catalysis in Chemistry and Enzymology*, pp 358–360, Dover, New York.
- Jones, T. A. (1985) *Methods Enzymol.* 115, 157–171.
- Kabsch, W. (1988) *J. Appl. Crystallogr.* 21, 916–924.
- Krieger, M., Kay, L. M., & Stroud, R. M. (1974) *J. Mol. Biol.* 83, 209–230.
- Perona, J. J., Tsu, C. A., Craik, C. S., & Fletterick, R. J. (1993a) *J. Mol. Biol.* 230, 919–933.
- Perona, J. J., Tsu, C. A., McGrath, M. E., Craik, C. S., & Fletterick, R. J. (1993b) *J. Mol. Biol.* 230, 934–949.
- Perona, J. J., Evnin, L. B., & Craik, C. S. (1994) *Gene* (in press)
- Phillips, M. A., Fletterick, R. J., & Rutter, W. J. (1990) *J. Biol. Chem.* 265, 20692.
- Phillips, M. A., Hedstrom, L., & Rutter, W. J. (1992) *Protein Sci.* 1, 517.
- Ruhmann, A., Kukla, D., Schwager, P., Bartels, K., & Huber, R. (1973) *J. Mol. Biol.* 77, 417–436.
- Schechter, I., & Berger, A. (1968) *Biochem. Biophys. Res. Commun.* 27, 157.
- Smith, H. B., & Hartman, F. C. (1991) *Biochemistry* 30, 5172–5177.
- Toney, M. D., & Kirsch, J. F. (1989) *Science* 243, 1485–1488.
- Zerner, B., Bond, R. P. M., & Bender, M. L. (1964) *J. Am. Chem. Soc.* 86, 3669.
- Zhukovsky, E. A., Robinson, P. R., & Oprian, D. D. (1991) *Science* 251, 558–560.